Wind Estimation in the Lower Atmosphere Using Multirotor Aircraft

ROSS T. PALOMAKI, NATHAN T. ROSE, MICHAEL VAN DEN BOSSCHE, THOMAS J. SHERMAN, AND STEPHAN F. J. DE WEKKER

Department of Environmental Sciences, University of Virginia, Charlottesville, Virginia

(Manuscript received 13 September 2016, in final form 19 March 2017)

ABSTRACT

Unmanned aerial vehicles are increasingly used to study atmospheric structure and dynamics. While much emphasis has been on the development of fixed-wing unmanned aircraft for atmospheric investigations, the use of multirotor aircraft is relatively unexplored, especially for capturing atmospheric winds. The purpose of this article is to demonstrate the efficacy of estimating wind speed and direction with 1) a direct approach using a sonic anemometer mounted on top of a hexacopter and 2) an indirect approach using attitude data from a quadcopter. The data are collected by the multirotor aircraft hovering 10 m above ground adjacent to one or more sonic anemometers. Wind speed and direction show good agreement with sonic anemometer measurements in the initial experiments. Typical errors in wind speed and direction are smaller than 0.5 m s^{-1} and 30°, respectively. Multirotor aircraft provide a promising alternative to traditional platforms for vertical profiling in the atmospheric boundary layer, especially in conditions where a tethered balloon system is typically deployed.

1. Introduction

Investigating atmospheric boundary layer flows is limited by the difficulty of making detailed wind observations in the lower atmosphere. A common method of in situ data collection in the lowest few hundred meters uses a sensor package with a cup and vane anemometer attached to a tethered balloon [for recent studies using this method, see, e.g., Lehner et al. (2015) and Kalverla et al. (2016)]. Operating the tethered balloon system via the tether line and winch, inflating the balloon, attaching the sensor package on the tether, and handling the balloon can be challenging and labor intensive. Furthermore, the tethered balloon system and the required helium are expensive. Unmanned aerial vehicles (UAVs) provide an alternative platform for data collection in the lower atmosphere. The versatility of UAVs has led to a rapid increase in their use in environmental studies and meteorology (Anderson and Gaston 2013; Guest and Machado 2014). Applications for atmospheric research have mostly been limited to the use of fixed-wing UAVs (Martin et al. 2011; Mayer et al. 2012; Van den Kroonenberg et al. 2012; Lawrence and Balsley 2013). Wind velocity estimation using a fixed-wing UAV requires the UAV to travel horizontally for some distance (e.g., Van den Kroonenberg et al. 2008), thereby making it impractical to measure vertical wind profiles or the temporal variability of the wind at one point in space.

In recent years, rotary-wing UAVs, also referred to as multirotor aircraft or copters, have been used for applications such as aerial imagery, but their application in atmospheric research has been mostly absent in scientific literature. Advantages of multirotor copters include their vertical takeoff and landing capability and their ability to hover at a fixed point. These advantages make the multirotor copter an ideal platform to measure vertical profiles or to obtain temporal changes of meteorological variables at a fixed location. Multirotor copters are a potential replacement for balloon-based systems because they are low cost, easy to operate, durable in a wide range of atmospheric conditions, and reusable. Having such a reliable and repeatable method for atmospheric data collection will allow for detailed investigations of the structure and dynamics of the lower atmosphere.

Much of the extensive literature on multirotor copters focuses on efforts to optimize controlled maneuverability (e.g., Hoffmann et al. 2007, 2008, 2011; Nicol et al. 2011). Several studies (Waslander and Wang 2009; Chen et al. 2013; Schiano et al. 2014) consider the effect of wind as an interference to overcome with an improved flight

Corresponding author: Stephan F. J. De Wekker, dewekker@virginia.edu

DOI: 10.1175/JTECH-D-16-0177.1

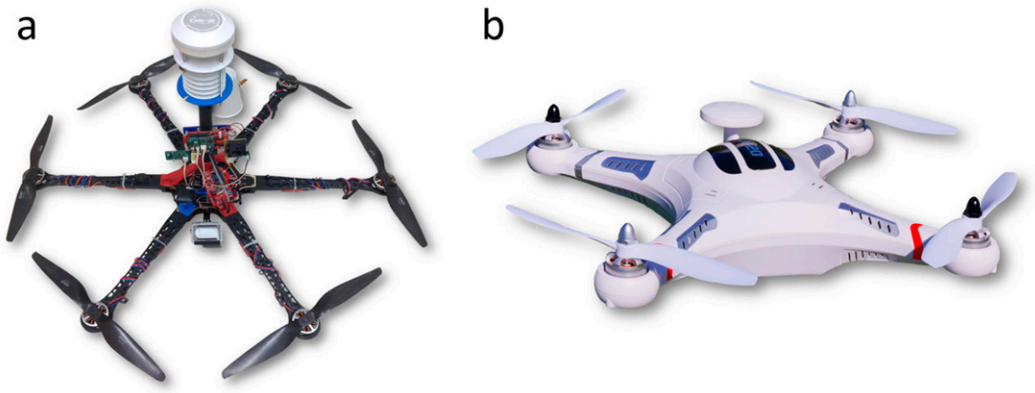

FIG. 1. (a) Hexacopter used in the direct method. (b) Quadcopter used in the indirect method.

controller. More recently, Neumann and Bartholmai (2015) made an initial attempt to use a quadcopter for estimating winds using attitude data (roll and pitch). Their wind estimates using this indirect approach showed good agreement with independent wind measurements, but the relationship between wind speed and attitude was derived using a wind tunnel, which may not be easily accessible for researchers. We follow up on this approach by deriving this relationship by using only data collected in the field. Additionally, we apply a direct approach by mounting a sonic anemometer on a multirotor copter to make wind measurements.

Here, we focus on the estimate of wind speed and direction from a hovering multirotor copter with both the direct and indirect approaches and compare these estimates with independent wind measurements from sonic anemometers. The remainder of this paper is organized as follows: Section 2 introduces the experimental methods, which include a physical model of the quadcopter used for the indirect method. Results are presented in section 3, followed by a discussion of the uncertainties, issues, and needs for future work in section 4. Concluding remarks are made in section 5.

2. Methodology

Flights for testing both the direct and indirect approaches took place outdoors in the foothills of the Blue Ridge Mountains near Charlottesville, Virginia. The test site was an open farm field with gently rolling hills. Test flights for the direct and the indirect approaches were performed on 3 June 2014 and 2 August 2015, respectively, under partly cloudy and weakly unstable conditions, with wind gusts peaking at just under 5 m s^{-1}. Since our focus is on the use of a multirotor copter in place of a tethered balloon system, we conducted our test flights under conditions suitable for balloon operations.

a. Direct approach

For the direct approach we used a hexacopter with a large carrying capacity and fail-safe six-motor design (Fig. 1a). The hexacopter had a 550-mm motor-to-motor diameter frame (DJI Flame Wheel F550) with 38-cm propellers. A flight controller (3D Robotics PixHawk) was used with ArduCopter firmware. The payload consisted of a 500-g 2D sonic anemometer (Decagon Devices DS-2) attached on top of the hexacopter via a 30-cm pole. During the flight, data were collected at 1 Hz using an Arduino datalogger. Independent wind data were obtained from a 3D sonic anemometer (Gill WindMaster) atop a 10-m tower.

Prior to the outdoor test flights, indoor testing was performed in a basketball arena to investigate the effect of the rotors on wind measurements taken 30 cm above the copter. The copter and the attached sonic anemometer were flown 5 m away from a tower with an identical anemometer. Both anemometers were sampling 6 m above the stadium floor. A comparison of the measurements (not shown) indicated that the mean increase of the wind speed measured by the copter anemometer was 0.5 m s^{-1} when compared to the tower anemometer, which sampled the undisturbed flow. This bias was subtracted from the direct approach wind speed measurements in further analyses.

b. Indirect approach

For the indirect approach, a quadcopter (Quanum Nova) was used with a 300-mm motor-to-motor diameter frame (Fig. 1b). This quadcopter was controlled by a flight controller (APM, version 2.52) using ArduCopter firmware. The flight controller uses an MPU-6000 inertial measurement unit (IMU) in conjunction with an L883 three-axis digital compass. The IMU uses accelerometers and gyroscopes to calculate pitch and roll angles and calculates the yaw angle from

the digital compass measurements. The attitude data were recorded at 10 Hz. Independent wind data were obtained at the outdoor field site using 2D sonic anemometers (Decagon Devices DS-2) atop three 10-m towers that were positioned in a triangular configuration approximately 13 m apart. We made these measurements in this configuration to obtain some estimate of the wind speed variability within an area of about 75 m^2. Data from the three anemometers were recorded at 1 Hz with GPS time to ensure proper synchronization between towers. An examination of the anemometer data indicated that one of the anemometers was slightly misaligned during the site setup and exhibited a mean bias of 16.9° compared to the other anemometers. This bias was subsequently removed from the direction measurements of the affected anemometer.

The quadcopter was controlled manually to a height of 10 m in the center of the triangle, and the yaw angle was set to 0° (magnetic north). At that point, the flight mode was switched to "GPS hold" mode and the quadcopter maintained this position using GPS coordinates. After 7–10 min of hover time, the quadcopter was manually landed at its launch point. Only data from the hover period are used in subsequent analyses.

The basis for the indirect approach is a simplified model of a quadcopter. In this model, three main forces act on the quadcopter system: thrust $\mathbf{T}$, drag $\mathbf{D}$, and gravitational force $\mathbf{G}$ (see, e.g., Seddon and Newman 2011). Let $\mathbf{e}_N, \mathbf{e}_E$, and $\mathbf{e}_D$ be unit vectors in the north–east–down inertial coordinates and $\mathbf{X}_B, \mathbf{Y}_B$, and $\mathbf{Z}_B$ be the unit vectors along the quadcopter's body axes. Roll (φ), pitch (θ), and yaw (ψ) are rotations that parameterize a rotation matrix that maps the quadrotor's body frame to the fixed inertial frame (Etkin 1972). When the φ, θ, and ψ rotations are small, they can be approximated as rotations about the $\mathbf{e}_N, \mathbf{e}_E$, and $\mathbf{e}_D$ axes, respectively, as illustrated in Fig. 2. We assume that the roll, pitch, and yaw rotations are small, and that the plane of each rotor is parallel to the $\mathbf{X}_B - \mathbf{Y}_B$ plane. Thus, the total force acting on the quadcopter system is

$$\mathbf{F} = \mathbf{G} + \mathbf{D} + \mathbf{T} = mg\mathbf{e}_D - D\mathbf{e}_v - \sum_{i=1}^{4} \mathbf{T}_i \qquad (1)$$

where $mg\mathbf{e}_D$ is the gravitational force along the inertial $\mathbf{e}_D$ axis, $D\mathbf{e}_v$ is the drag force opposite of the relative wind velocity $\mathbf{e}_v$ in inertial coordinates, and $\mathbf{T}_i$ is the thrust in the direction perpendicular to the plane of the ith rotor. In an ideal hover, forces are balanced and the thrust force equals the combination of drag force and gravity as

$$\mathbf{T} = mg\mathbf{e}_D - D\mathbf{e}_v. \qquad (2)$$

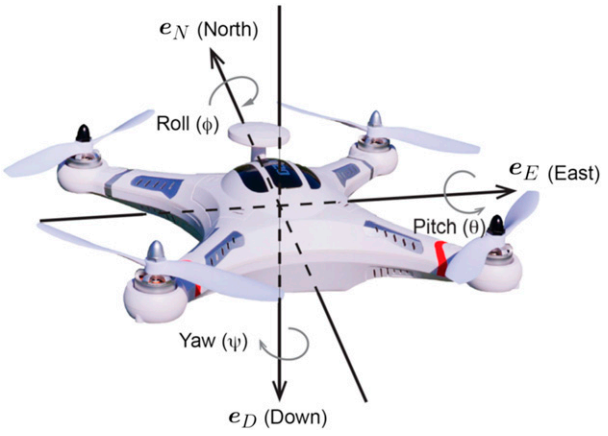

FIG. 2. Axes system on the quadcopter used for the indirect method. For small angles, roll (ϕ), pitch (θ), and yaw (ψ) are rotations about the $\mathbf{e}_N$, $\mathbf{e}_E$, and $\mathbf{e}_D$ axes, respectively. In the positioning above, the quadcopter's body axes (not shown) align with the inertial axes.

In the absence of wind, the system does not experience any drag force and the thrust force opposes only the force of gravity, that is, $\mathbf{T} = mg$. Forces in this scenario act only along $\mathbf{e}_D$. When wind (and therefore drag) is introduced into the system, the quadcopter tilts and $\mathbf{T}$ no longer aligns with the negative $\mathbf{e}_D$ axis. This tilt angle α between $\mathbf{T}$ and $-\mathbf{e}_D$ (the up direction) is a combination of the roll and pitch angles. If the introduced wind is horizontal, that is, $\mathbf{e}_v$ lies on the $\mathbf{e}_N - \mathbf{e}_E$ plane and has both vertical and horizontal components:

$$\mathbf{T} = \mathbf{T}_v\mathbf{e}_v + \mathbf{T}_D\mathbf{e}_D = |\mathbf{T}|\sin\alpha\mathbf{e}_v + |\mathbf{T}|\cos\alpha\mathbf{e}_D. \qquad (3)$$

Combining (2) and (3),

$$|\mathbf{T}|\sin\alpha = \mathbf{D} \qquad (4)$$

$$|\mathbf{T}|\cos\alpha = mg. \qquad (5)$$

A slight rearrangement to the ratio of (4) and (5) leads to a new definition of the drag force,

$$\mathbf{D} = mg\tan\alpha. \qquad (6)$$

The classic Raleigh drag equation of an object in air takes into account the object's drag coefficient C_D, air density ρ, the object's exposed area A, and the square of the relative wind velocity v,

$$\mathbf{D} = \frac{1}{2}C_D\rho A v^2. \qquad (7)$$

We assume that a hovering copter does not move inertially and take the relative wind velocity to be the measured wind velocity. When applying (7) to the

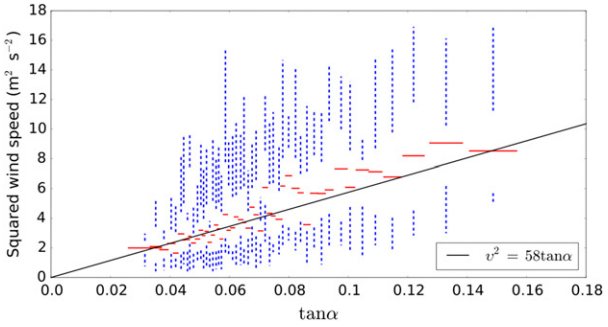

FIG. 3. Squared wind speed as a function of tanα. Data from flights 1, 3, and 4 were binned to determine $\hat{c}$. Each bin contains 50 data points and is plotted as a standard box plot, with the box enclosing the area around the first and third quartiles removed for clarity. Dashed whiskers extend 1.5 times the interquartile range below the first quartile and above the third quartile.

quadcopter in hover, several of the variables prove difficult to calculate. The general shape of the quadcopter is very nonaerodynamic, and the layout of its frame, rotors, and landing supports make a geometric approximation for a numerical drag coefficient ineffective. Additionally, A constantly changes as the quadcopter's tilt varies throughout the flight. The semipermeability of the rotating propellers, which is a function of the rotations per minute, further exacerbates the difficulty of calculating A at a given point in time (Gonzalez-Rocha et al. 2017). To avoid these difficulties, we combine (6) and (7) as

$$v^2 = \hat{c}\tan\alpha, \tag{8}$$

where $\hat{c}$ is an empirically determined coefficient that implicitly includes $m, g, \rho, A,$ and C_D. The tilt angle α is calculated using the quadcopter's roll and pitch angles,

$$\alpha = \arccos(\cos\theta\cos\phi). \tag{9}$$

The numerical value of $\hat{c}$ was determined by first plotting the tangent of the tilt angle against the square of anemometer-collected wind speed at each time stamp for three of the four flights. The quadcopter attitude data were originally collected at 10 Hz and resampled at 1 Hz to match the anemometer time series. Equation (9) was used to derive α from the recorded φ and θ data. The α angle data were sorted into 50 bins with an equal number of observations in each bin, and a linear regression through the origin was computed using the binned medians. The value of $\hat{c}$ was then used to estimate the wind speed during the independent fourth flight. An example is shown in Fig. 3, where a linear regression of the binned data from flights 1, 3, and 4 yielded a value for $\hat{c}$ of 58, with a standard error for $\hat{c}$ of 2. Note that forcing the regression through the origin may artificially decrease the standard error compared to a regression where the intercept is not forced (Freund et al. 2006). The calculated $\hat{c}$ was used with (8) and the tilt angles from flight 2 to derive the estimate of wind speed (shown later in Fig. 5).

With the quadcopter's yaw angle set to 0°, wind direction λ is estimated with a geometric approach using the quadrotor's roll and pitch angles,

$$\lambda = \arctan\left(\frac{-\sin\phi\cos\theta}{\cos\phi\sin\theta}\right) + 180°. \tag{10}$$

The 180° correction allows the direction to be reported as the angle from which the wind originates. If setting the yaw angle to 0° is not possible, then an algorithm to determine wind direction from another heading can be found in Neumann and Bartholmai (2015).

3. Results

For both methods, results are presented with the raw 1-Hz data in addition to data smoothed with a 10-s moving average. This 10-s window was chosen for ease of comparison and for taking into account several uncertainties related to the collection of wind data, including the response time of the copter to external disturbances (relevant for the indirect approach) and the synchronization of the time on the various instruments. All discussion and analyses of the data below refer to the smoothed data.

a. *Direct approach*

Figure 4 shows an example of the comparison between the winds from the sonic anemometer on the hexacopter and the independent wind measurement from the tower at 10-m height AGL. Winds fluctuated between 1 and 5 m s^{-1} and between 270° and 360° during the ~ 500-s period. For this particular flight (flight 4), the RMSE in wind speed was 0.67 m s^{-1} and 25° in wind direction. The RMSE and bias values are presented in Table 1. For all four flights, RMSE ranged between 0.27 and 0.67 m s^{-1} for wind speed. RMSE values for wind direction were between 25° and 56°. Wind speed and direction biases were positive at about 0.1 m s^{-1} and 10°, respectively, averaged over all flights.

Fluctuations in wind speed and direction of a few meters per second and a few tens of degrees were captured well by the hexacopter's sonic anemometer, for example, the periods between 350 and 410 s for wind speed and between 100 and 200 s for wind direction (Fig. 4). However, there were occasions when the copter anemometer overestimated the wind speed by approximately 1 m s^{-1},

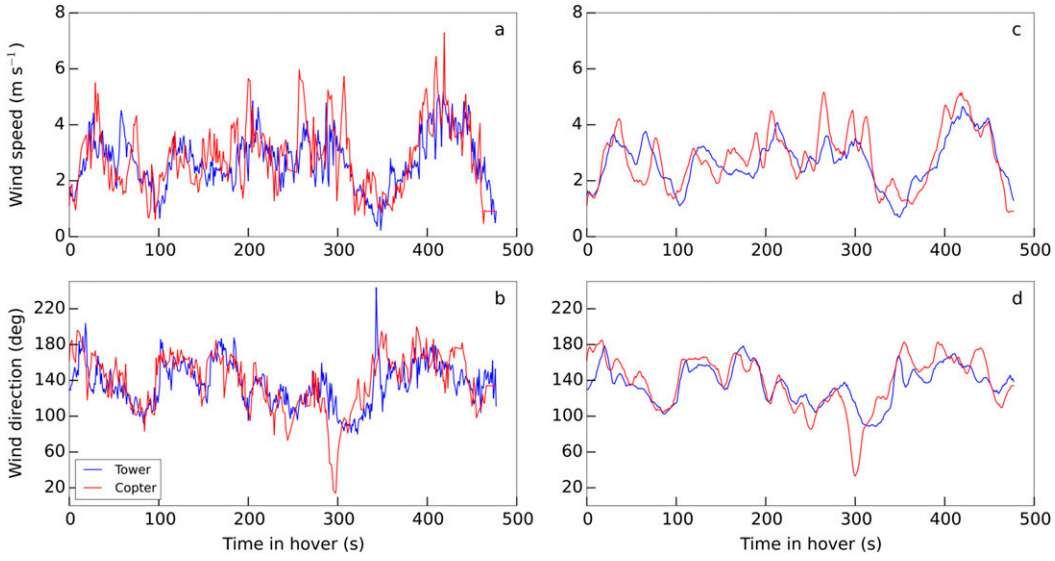

FIG. 4. Estimations of 1 s of 10-m (a) wind speed and (b) wind direction, and 10-s estimations of (c) wind speed and (d) wind direction during flight 4 on 3 Jun 2014 using the direct approach (red line) compared with the independent sonic measurement atop a 10-m tower (blue line). To facilitate the plotting and analysis, 180° was subtracted from the actual wind direction.

including on three occasions between 270 and 310 s (Fig. 4). It was also during this period that the wind direction deviated the most from the independent wind measurement. During the hover, we visually observed instances during which the copter was not stable, that is, there were slight horizontal and vertical jerking movements that could produce wind speed and direction deviations. Later examination of the flight logs showed that horizontal velocities recorded by the GPS sensor and the onboard accelerometer were on the order of 0.2 m s^{-1} and had some discrepancies. Differences between the two sensors were typically about 0.3 m s^{-1} and at times approached 0.5 m s^{-1}. Although we cannot pinpoint the exact cause for these differences, they may be due to changes in the GPS signal quality during the hover period. Over the course of the flight, the number of satellites being used by the GPS sensor ranged from 8 to 12.

b. *Indirect approach*

Figure 5 shows the comparison between winds estimated using the indirect method and independent wind measurements at 10-m height AGL. Winds varied between 1 and 4 m s^{-1} and between 120° and 200° during this particular flight (flight 2). The gray shading in this figure illustrates the range of the wind speeds and directions measured on the three towers that surrounded the hovering copter. This range provides an estimate of the variability of the winds within this $\sim 75\,m^2$ area of the atmosphere. The wind variability was occasionally quite large with wind speed differences of nearly 1 m s^{-1} and wind direction differences of approximately 40° between the towers. For all flights, the RMSE for each individual tower anemometer compared to the mean value of all three tower anemometers varied between 0.2 and 0.3 m s^{-1} for wind speed and 5°–10° for wind direction (not shown). In comparison, the RMSE for the quadcopter-estimated wind compared to the mean anemometer values varied between 0.3 and 0.9 m s^{-1} and 10° and 21° (Table 2), respectively. For the results from flight 2 (Fig. 5), the RMSE values are 0.36 m s^{-1} for wind speed and 11° for wind direction (Table 2). The wind estimate from the quadcopter generally fell within the measured range of wind speeds and directions, but there were occasions with under- or overestimations of wind speed of up to 1 m s^{-1} and of wind direction up to 20°. Wind speed and direction biases were negative at about 0.2 m s^{-1} and 10°, respectively, averaged over all flights (Table 2).

TABLE 1. RMSE and bias values for wind speed and direction estimated using the direct approach for all flights.

	Speed (m s^{-1})		Direction (°)	
Flight	RMSE	Bias	RMSE	Bias
1	0.27	0.14	29	22
2	0.39	0.00	56	−13
3	0.63	0.05	46	32
4	0.67	0.12	25	−6

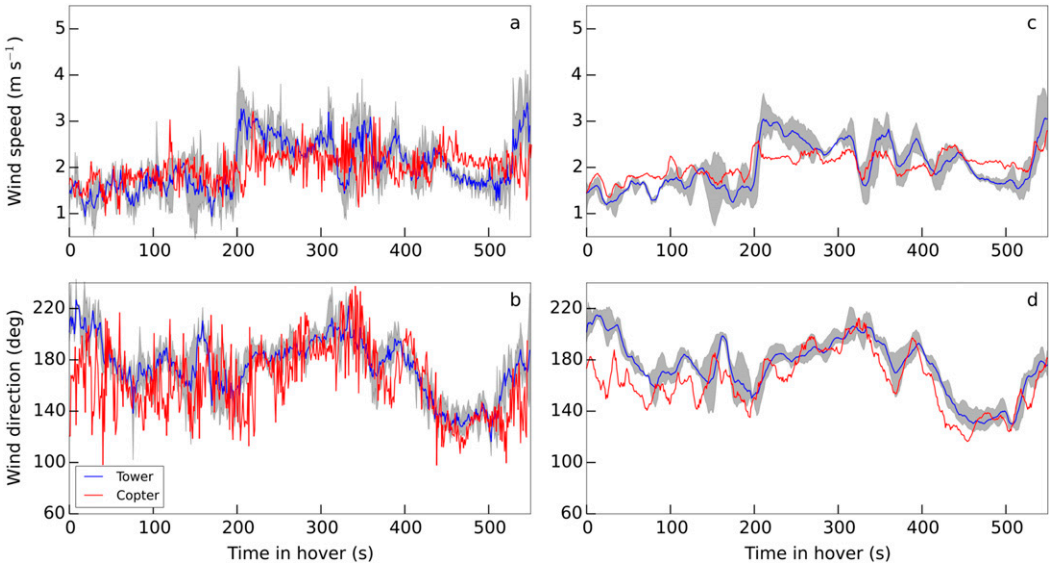

FIG. 5. Estimations of 1 s of 10-m (a) wind speed and (b) wind direction, and 10-s estimations of (c) wind speed and (d) wind direction during flight 2 on 2 Aug 2015 using the indirect approach (red line) compared with the mean wind speed of the anemometers atop the three 10-m towers (blue line). Shading outlines the range of the wind speed and direction values measured atop the three towers.

4. Discussion

While the results of this exploratory study suggest that multirotor copters are a promising platform for the observation of winds, we also recognize that there are many uncertainties and potential issues, especially regarding the accuracy of the observations.

Our results indicate that the direct and indirect approaches can estimate wind speed with similar accuracy, and that wind direction is more accurately estimated by the indirect approach. Table 2 shows that for three of the four flights, the RMSE for wind direction is between 10° and 14°. Differences of this order of magnitude are observed when the individual tower anemometers are compared to the mean of the three anemometers. Figure 5 shows several periods of 15 s or longer where the tower measurements of wind direction differ by more than 20° from the estimated winds, including one period when measurements differ by more than 40°.

For the indirect method, we note in Table 2 large biases in wind direction for flight 1 and in wind speed for flight 4. We also calculated the so-called variable error (defined similarly as the RMSE but with the difference of the bias-adjusted copter estimate with respect to the anemometer mean), which was similar among all flights. The large biases can therefore explain the large RMSEs for wind direction in flight 1 and for wind speed in flight 4. We also note that in these cases, a large bias in either the estimated wind speed or direction does not necessarily mean that both variables are biased. For example, there is zero bias in wind direction in flight 4, even though it had the largest recorded wind speed bias. A better understanding of why these biases occur will help to make more accurate wind estimates.

RMSE and bias values presented in Tables 1 and 2 are averaged over the entire hover duration. For vertical profiling applications, it may be more practical to calculate these figures over shorter periods. For the direct method, the wind speed RMSEs calculated for 10-s periods during flight 4 (Fig. 4) had a mean value of 0.58 ± 0.31 m s^{-1}, with a minimum of 0.15 m s^{-1} and a maximum of 1.62 m s^{-1}. The wind direction RMSE calculated for 10-s periods had a mean value of 15° ± 12°, with a minimum of 2° and a maximum of 59°. For the indirect method, the wind speed RMSE calculated for 10-s periods during flight 2 (Fig. 5) had a mean value of 0.32 ± 0.17 m s^{-1}, with a minimum of 0.07 m s^{-1} and a maximum of 0.77 m s^{-1}. The wind direction RMSE calculated for 10-s periods had a mean value of 11 ± 7°, with a minimum of 2° and a maximum of 39°. While these

TABLE 2. RMSE and bias values for wind speed and direction estimated using the indirect approach for all flights.

	Speed (m s^{-1})		Direction (°)	
Flight	RMSE	Bias	RMSE	Bias
1	0.31	−0.09	21	−20
2	0.36	0.02	14	−6
3	0.49	0.17	10	−4
4	0.88	−0.77	12	0

RMSE values are comparable to the RMSE values over the entire hover period, the range of these values for 10-s periods is large. Figures 4 and 5 indeed show some periods when the estimates are quite close to the true values and other periods when the estimate deviates considerably. The smaller standard deviations for the RMSEs for the indirect method indicate that this method produced more consistent estimates in our testing conditions.

The rotors of the copter had an effect on the wind estimates from the copter-mounted anemometer in the direct approach. From an indoor test, we estimated an average positive bias due to the rotors of about 0.5 m s^{-1}. We subtracted this bias from the outdoor flight data. The remaining wind speed bias averaged over all flights was only slightly positive at about 0.1 m s^{-1}, providing confidence that a correction of 0.5 m s^{-1} for this particular frame and anemometer setup was reasonable. Even with this bias removed, the mounted anemometer does sample a wind field disturbed by the rotors. The turbulent nature of this disturbance may cause discrepancies in wind speed and wind direction, especially during slight downward motions of the hexacopter. Additionally, larger copter tilt angles could result in underestimations of the wind by the 2D sonic anemometer, since it is no longer level with respect to mean sea level. During our test flights in relatively calm conditions, the largest tilt angle recorded was approximately 20°; wind speed measurements taken at this angle could have an error of more than 6%. One possible approach to avoid this issue is to mount a 3D sonic on the copter that can measure the total wind speed at any copter tilt angle.

We recognize that reducing the relationship between wind speed and tilt to the determination of a constant $\hat{c}$ is a simplification of the physical quadcopter system. In particular, the A and C_D parameters present in $\hat{c}$ may not be constant during the entire test flight. As previously discussed, these two terms are difficult to determine accurately using only field measurements. Additionally, these two parameters may depend on the wind speed itself. For example, the exposed area A would increase at higher wind speeds, due to the increased tilt angle of the copter. While we have determined $\hat{c}$ from a relationship between the tilt and the square of the wind speed that results from the theory, we also experimented with determining $\hat{c}$ from a binned linear regression of $\tan\alpha$ against linear wind speed. Doing so resulted in wind speed estimations and RMSE values that were close to those shown in Table 2. Neumann and Bartholmai (2015) used quadratic and cubic functions for the relationship between wind speed and quadcopter tilt angle obtained from experiments in a wind tunnel. However, in their figures, the relationship is rather linear up to wind speeds of about 5 m s^{-1}, similar to what we find in our experiments.

The wind speed estimation using the indirect method was able to capture some but not all of the wind variability, and there are times with large discrepancies between the estimated and measured winds. We examined other variables in the flight controller output in an attempt to determine the cause of these discrepancies. As mentioned previously, the number of satellites used by the GPS sensor fluctuated during hover periods, which may have introduced discrepancies into the recorded velocity measurements. Higher accuracy position determination, for example using differential GPS, will minimize the risk of introducing these errors. Anomalies in other data from the flight controller, including position, velocity, and acceleration, did not consistently align in time with the estimation discrepancies, and we were unable to conclude that any of these variables could reliably determine the outliers. Additionally, it is difficult to determine whether a spike in copter velocity or acceleration is due to a wind gust or to an issue with any sensor on the onboard flight computer. We suggest filming future test flights, as video evidence could serve as a reference to help determine the source of any erratic behavior that appears during data postprocessing.

The wind speed estimation using the indirect method was relatively insensitive to the number of bins used in the regression process. For each independent flight, we examined several additional regressions using bins ranging from 25 to 50 data points per bin. The slope of the regression line changed by 10% or less for each flight, which resulted in a change in the RMSE of the estimation by 5% or less for each flight. We also performed regressions where the intercept was not forced through the origin. The majority of our regressions had intercepts very close to zero, indicating that our assumptions of balance in the physical quadcopter model are close to reality.

The slope of the regression line was within 20% for all our flights. This suggests that although $\hat{c}$ depends on several properties that are not necessarily constant (as discussed previously), its value is relatively constant across flights. This enables us to determine $\hat{c}$ for a particular multirotor copter and, subsequently, use it to estimate wind speeds without further calibration. Additional test flights in a wider range of wind speeds and with different multirotor copters will provide more insight into this hypothesis. We believe that development of postprocessing techniques to improve quality control of the data could further decrease uncertainties in determining $\hat{c}$.

Our test flights to collect wind data consisted only of hovering flight patterns. Future tests should investigate a

variety of flight strategies for obtaining vertical wind profiles, including constant ascent and descent rates with a single copter, and multiple vertically stacked copters. These profiles can then be compared with profiles from, for example, radiosondes, tethersondes, and Doppler lidar to characterize the limitations and uncertainties of vertical wind profiles collected with a copter. Furthermore, wind estimates might be improved by using different hardware and software options. In particular a stable hover is important for accurate wind observations. The hover characteristics are dependent on many factors, including the weight and diameter of the multirotor frame, the quality of the GPS signal, and various tuning parameters that differ between copter designs. Changing certain tuning parameters [such as the proportional–integral–derivative (PID) controller gains] could also improve the responsiveness of the copter to wind gusts, allowing higher-frequency wind measurement.

In summary, our preliminary results indicate that multirotor copters show potential to measure atmospheric winds in light to moderate conditions. However, additional studies are desired before our direct and indirect methods can be used to make vertical profiles of the atmosphere in situations when a tethered balloon would traditionally be deployed. For the direct method, the influence of ambient winds, copter frame, height of the anemometer above the copter frame, and rotor characteristics need to be further investigated. For the indirect method, more accurate measurements of the exposed area and drag coefficient are needed to better constrain the relationship between tilt and wind speed, as defined by $\hat{c}$. More experiments are also needed to determine the accuracy of the direct and indirect wind estimates at higher wind speeds.

5. Conclusions

We estimated atmospheric winds from a multirotor copter with a direct approach using a copter-mounted sonic anemometer, and with an indirect method using a theoretically derived tilt–wind relationship. Both approaches had typical RMSEs of about 0.5 m s^{-1} and 30° when compared with independent wind measurements in calm to moderate conditions (0–5 m s^{-1}) for the duration of the flight (~ 8 min). When the flight duration is divided into smaller periods—for example, 10 s—the mean of these 10-s RMSE values is comparable to the RMSE value for the entire flight duration. The standard deviations of the 10-s RMSE values are larger for the direct method than for the indirect method. Wind speed biases are smaller for the direct method than for the indirect method, while wind direction biases are smaller for the indirect method than for the direct method. The measurement uncertainty can be further reduced by improvements in hardware and software options as well as postprocessing procedures. We conclude that the multirotor platform provides a promising low-cost alternative to traditional platforms for vertical profiling in the atmospheric boundary layer.

Acknowledgments. This research was partially funded by NSF Award ATM-1151445 and by Office of Naval Research Award N00014-11-1-0709. We thank Doug Chestnut, Gianluca Guadagni, Greg Lewin, John Porter, and especially Craig Woolsey for the stimulating discussions related to this research. We also thank three reviewers for their valuable comments, which improved the manuscript.

REFERENCES

Anderson, K., and K. Gaston, 2013: Lightweight unmanned aerial vehicles will revolutionize spatial ecology. *Front. Ecol. Environ*, **11**, 138–146, doi:10.1890/120150.

Chen, Y., Y. He, and M. Zhou, 2013: Modeling and control of a quadrotor helicopter system under impact of wind field. *Res. J. Appl. Sci. Eng. Technol.*, **6**, 3214–3221.

Etkin, B., 1972: *Dynamics of Atmospheric Flight*. Dover Publications, 579 pp.

Freund, R. J., W. J. Wilson, and P. Sa, 2006: *Regression Analysis: Statistical Modeling of a Response Variable*. 2nd ed. Academic Press, 480 pp.

Gonzalez-Rocha, J., C. A. Woolsey, C. Sultan, N. Rose, and S. F. J. De Wekker, 2017: Measuring atmospheric winds from quadrotor motion. *Proc. AIAA Atmospheric Flight Mechanics Conference/AIAA SciTech Forum*, Denver, CO, American Institute of Aeronautics and Astronautics, AIAA 2017-1189, doi:10.2514/6.2017-1189.

Guest, P., and C. Machado, 2014: Using UAS to sense the physical environment and predict electromagnetic system performance. Naval Postgraduate School Tech. Rep. NPS-MR-15-001, 78 pp.

Hoffmann, G., H. Huang, S. Waslander, and C. Tomlin, 2007: Quadrotor helicopter flight dynamics and control: Theory and experiment. *Proc. AIAA Guidance, Navigation, and Control Conf.*, Hilton Head, SC, American Institute of Aeronautics and Astronautics, AIAA 2007-6461, doi:10.2514/6.2007-6461.

——, S. Waslander, and C. Tomlin, 2008: Quadrotor helicopter trajectory tracking control. *Proc. AIAA Guidance, Navigation, and Control Conf. and Exhibit*, Honolulu, HI, American Institute of Aeronautics and Astronautics, AIAA 2008-7410, doi:10.2514/6.2008-7410.

——, H. Huang, S. Waslander, and C. Tomlin, 2011: Precision flight control for a multi-vehicle quadrotor helicopter testbed. *Control Eng. Pract.*, **19**, 1023–1036, doi:10.1016/j.conengprac.2011.04.005.

Kalverla, P. C., G.-J. Duine, G.-J. Steeneveld, and T. Hedde, 2016: Evaluation of the Weather Research and Forecasting Model in the Durance valley complex terrain during the KASCADE Field Campaign. *J. Appl. Meteor. Climatol.*, **55**, 861–882, doi:10.1175/JAMC-D-15-0258.1.

Lawrence, D., and B. Balsley, 2013: High-resolution atmospheric sensing of multiple atmospheric variables using the DataHawk

small airborne measurement system. *J. Atmos. Oceanic Technol.*, **30**, 2352–2366, doi:10.1175/JTECH-D-12-00089.1.

Lehner, M., C. D. Whiteman, S. W. Hoch, D. Jensen, E. R. Pardyjak, L. S. Leo, S. Di Sabatino, and H. J. S. Fernando, 2015: A case study of the nocturnal boundary layer evolution on a slope at the foot of a desert mountain. *J. Appl. Meteor. Climatol.*, **54**, 732–751, doi:10.1175/JAMC-D-14-0223.1.

Martin, S., J. Bange, and F. Beyrich, 2011: Meteorological profiling of the lower troposphere using the research UAV "M^2AV Carolo." *Atmos. Meas. Tech.*, **4**, 705–716, doi:10.5194/amt-4-705-2011.

Mayer, S., A. Sandvik, M. Jonassen, and J. Reuder, 2012: Atmospheric profiling with the UAS SUMO: A new perspective for the evaluation of fine-scale atmospheric models. *Meteor. Atmos. Phys.*, **116**, 15–26, doi:10.1007/s00703-010-0063-2.

Neumann, P. P., and M. Bartholmai, 2015: Real-time wind estimation on a micro unmanned aerial vehicle using its internal measurement unit. *Sens. Actuators*, **235A**, 300–310, doi:10.1016/j.sna.2015.09.036.

Nicol, C., C. Macnab, and A. Ramirez-Serrano, 2011: Robust adaptive control of a quadrotor helicopter. *Mechatronics*, **21**, 927–938, doi:10.1016/j.mechatronics.2011.02.007.

Schiano, F., J. Alonso-Mora, K. Rudin, P. Beardsley, R. Siegwart, and B. Siciliano, 2014: Towards estimation and correction of wind effects on a quadrotor UAV. *Proc. IMAV 2014: Int. Micro Air Vehicle Conf. and Competition*, Delft, Netherlands, Delft University of Technology, 8 pp., doi:10.3929/ethz-a-010286793.

Seddon, J. M., and S. Newman, 2011: *Basic Helicopter Aerodynamics*. 3rd ed. Wiley, 286 pp.

Van den Kroonenberg, A., T. Martin, M. Buschmann, J. Bange, and P. Vörsmann, 2008: Measuring the wind vector using the autonomous mini aerial vehicle M^2AV. *J. Atmos. Oceanic Technol.*, **25**, 1969–1982, doi:10.1175/2008JTECHA1114.1.

——, S. Martin, F. Beyrich, and J. Bange, 2012: Spatially averaged temperature structure parameter over a heterogeneous surface measured by an unmanned aerial vehicle. *Bound.-Layer Meteor.*, **142**, 55–77, doi:10.1007/s10546-011-9662-9.

Waslander, S., and C. Wang, 2009: Wind disturbance estimation and rejection for quadrotor position control. *AIAA Infotech@Aerospace Conf.*, Seattle, WA, American Institute of Aeronautics and Astronautics, AIAA 2009-1983, doi:10.2514/6.2009-1983.